Quasiclassical Trajectory Study of Molecular Alignment Effects on the Dynamics of the Reactions of Cl, Br, and I with H_2

Miguel González,*,†,§ José D. Sierra,‡ Rafael Francia,‡ and R. Sayós*,‡,⊥

Departament de Química Física, Universitat de Barcelona, Martí i Franquès, 108028 Barcelona, Spain, and Departamento de Química, Universidad de La Rioja, Obispo Bustamante, 3. 26001 Logroño, Spain

Received: March 18, 1997; In Final Form: May 27, 1997⊗

The X + H_2 (X = Cl, Br, and I) reactions may be taken as models for endoergic triatomic reactions with heavy−light−light kinematics and collinear saddle point. The dependence of scalar and two-vector properties, angular distributions (**k**, **k′**), (**k**, **j′**), (**k′**, **j′**), and (**l′**, **j′**), on (E_T, v, j), as well as the effect of considering initial parallel (II), perpendicular (⊥), and random (null) **k**−**j** alignment has been studied using the quasiclassical trajectory (QCT) method. The threshold energy for II alignment is always higher than the ones for ⊥ and null alignments, but for high enough E_T values σ(II) becomes larger than σ(⊥) and σ(null), and the same occurs for the j-dependence. In the v range of values explored σ(II) is in general equal or larger than σ(⊥) and σ(null). The expression $^1/_3\sigma(\text{II}) + {}^2/_3\sigma(\perp)$ provides a very good estimate to σ(null) if the system is not in the vicinities of the threshold region, and some useful relations to simplify the QCT calculations for II alignment have also been given. For the two-vector properties considered, the results obtained for ⊥ alignment are in general closer to the ones for null alignment than the results obtained for II alignment. The angular correlations that result from the calculation are not a trivial result coming from a kinematic constraint; being particularly remarkable the role played by the rotation of the H_2 molecule. These results may be explained taking into account the saddle point properties, the "effective molecular size" of the rovibrationally excited H_2 molecule, and the geometrical implications of the alignments.

1. Introduction

Most of the experimental and theoretical efforts devoted to the understanding of the gas phase reaction dynamics have been focused on scalar properties, such as the total cross section and energy partitioning in products. In comparison with this, relatively little is known on properties that concern vectors of reactants and products, such as relative velocities and orbital and rotational angular momenta. Differing from scalars, vectors have not only magnitudes that are directly related with different types of kinetic energy (translational, orbital and rotational) but also directions. If the study of the reaction dynamics is restricted to scalar properties, it will not be possible to obtain full information on the forces that act in the reaction. In fact, although much more difficult to deal with, mainly from the experimental point of view, vector properties should also be considered in detail as they are key indicators of the anisotropy of the potential energy surface (PES) involved in the reaction. Hence, a complete understanding of the gas phase reaction dynamics is only possible after accounting for both type of properties together.[1−3] From these works, it becomes clear that the study of two-vector angular correlations among the set of vectors {**k**, **k′**, **j**, **j′**, **l**, **l′**}, where **k**, **l**, and **j** represent the initial (reactants) relative velocity, orbital angular momentum, and rotational angular momentum, respectively (primed variables refer to the final (products) vectors), is of great importance to the understanding of the dynamics of elementary chemical reactions (see also, for example refs 4 and 5).

The next set of reactions involved in the H_2X systems, being X an halogen atom (Cl, Br, and I), has been studied in this work using the quasiclassical trajectory (QCT) method:

$$\text{Cl} + \text{H}_2 \rightarrow \text{HCl} + \text{H}, \quad \Delta E = 0.13\ \text{eV} \tag{1}$$

$$\text{Br} + \text{H}_2 \rightarrow \text{HBr} + \text{H}, \quad \Delta E = 0.81\ \text{eV} \tag{2}$$

$$\text{I} + \text{H}_2 \rightarrow \text{HI} + \text{H}, \quad \Delta E = 1.55\ \text{eV} \tag{3}$$

where the reaction energy (ΔE) values have been derived from spectroscopic data.[6] This set of reactions may be taken as models for endoergic triatomic reactions with a PES that presents a collinear saddle point between reactants and products, and correspond to the H−L−L (heavy-light-light) kinematics.

In this work, mainly devoted to the stereodynamics of these reactions, the dependence of scalar properties (total cross section (σ) and average fraction of energies in products appearing as translation $\langle f_T' \rangle$, vibration $\langle f_V' \rangle$, and rotation $\langle f_R' \rangle$) and two-vector properties (angular correlations (**k**, **k′**), (**k**, **j′**), (**k′**, **j′**) and (**l′**, **j′**)) on relative translational energy (E_T), and rovibrational (v, j) levels of reactants, as well as the effect of considering initial perpendicular (⊥), parallel (II), and random (null) initial **k**−**j** alignment have been considered. Although the reactive scattering experiments required to study the effect of the initial **k**−**j** alignment are very difficult to carry out, see, for example, refs 1−2 and 7−8, and there is still a very scarce number of theoretical studies on this subject, see, for example, refs 8−10, this work highlights the interest of exploring the influence of reagents alignment to obtain a deeper insight into the dynamics and stereodynamics of elementary chemical reactions.

2. Analytical Potential Energy Surfaces

For the ground PES of the H_2Cl and H_2Br systems, respectively, the G3[11,12] and SEC[13] surfaces derived from Truhlar and co-workers have been used. In both cases, a modified LEPS surface with Sato parameters that depend on the three interatomic distances plus a three-center term localized

* To whom correspondence should be addressed.
† Universitat de Barcelona.
‡ Universidad de La Rioja.
§ E-mail: miguel@dynamics.qf.ub.es.
⊥ E-mail: r.sayos@dynamics.qf.ub.es.
⊗ Abstract published in *Advance ACS Abstracts,* September 15, 1997.

S1089-5639(97)00973-0 CCC: $14.00 © 1997 American Chemical Society

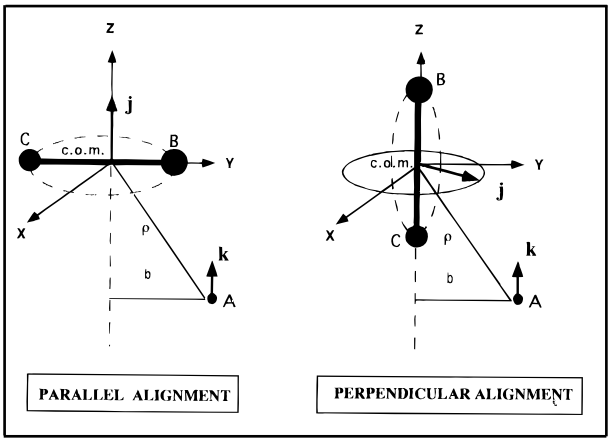

Figure 1. A + BC arrangements for initial parallel and perpendicular alignments.

at the collinear HXH saddle point, to make the surface more accurate in this region, was used to fit their ab initio electronic structure calculations on both PESs. Both surfaces have been tested[11,13] by comparing with experiments the calculated rate constants and kinetic isotope effects for the $H + HX \rightarrow H_2 + X$ (abstraction) and HX + H (exchange) reactions within the framework of the variational transition state theory with optimized multidimensional tunneling treatment (VTST/OMT). For reaction 1, a good agreement has been found recently between the measured differential cross section and the quantum mechanical and quasiclassical trajectory results.[12] For the H_2I system a new LEPS surface (hereafter indicated as the LEPS-65 PES) have been developed,[14] with Sato parameters $S_{IH} = S_{HH} = 0.125$ and the diatomics Morse parameters taken from ref 6. This surface has been derived by us from a LEPS based inversion (fitting)[14,15] of the experimental H_2 (v, j) rovibrational distributions arising from the $H + HI \rightarrow H_2 + I$ reaction.[16,17] The QCT calculations we have carried out on the LEPS-65 PES[15] reproduce quite well all experimental data, including also the H_2 ($v = 1$)/H_2 ($v = 0$) vibrational inversion.

3. Computational Details

Although the use of the QCT method to simulate gas-phase chemical reactions was established in the middle of the 1960s, this continues to be an active area of research.[18] Thus, it yields considerable and detailed information on the reaction kinetics and dynamics, often not available from other theoretical methods, with relatively simple means, if there exists an analytical fit of the PES, and the system is not very close to the threshold region, where quantum effects (mainly tunneling through the barrier) could play a dominant role. The three-dimensional (3D) QCT calculations have been carried out in a standard way, see, for example, refs 19 and 20, by means of the TRIQCT program.[21]

The selection of initial parallel or perpendicular alignments follows the same procedure employed in our previous work on the $K + HF \rightarrow KF + H$ reaction[10] and is represented in Figure 1. This figure shows both situations in the usual space-fixed right-handed coordinate system employed in trajectory calculations, which has the origin placed at the center of mass of the reagent diatomic molecule (BC), the attacking atom (A) placed in the *YZ* plane, and the relative velocity vector (**k**) pointing along the positive direction of the *Z* axis. For initial **k**−**j** parallel alignment, BC rotates in the *XY* plane, and its rotational angular momentum (**j**) may be directed along the positive or negative directions of the *Z* axis with equal probability. This corresponds to the two possible senses of BC rotation. For initial **k**−**j** perpendicular alignment, BC rotates in arbitrary planes perpendicular to the *XY* plane with **j** placed in the *XY* plane, all possible directions of **j** on this plane being equally probable. In the case of null (random) alignment, for each initial condition (E_T, v, j) it was checked that the initial **k**−**j** distribution was really isotropic. This means that the absolute values of the first and second Legendre moments $\langle P_1(\hat{\mathbf{k}}\cdot\hat{\mathbf{j}})\rangle$ and $\langle P_2(\hat{\mathbf{k}}\cdot\hat{\mathbf{j}})\rangle$, respectively) were very small (usually lower than 10^{-3} in absolute value).

For an arbitrary condition (E_T, v, j), the total energy for the two possible senses of BC rotation that correspond to the initial **k**−**j** parallel alignment is the same, but the total angular momentum vector **J** (**J** = **l** + **j**) is different in both cases. However, it is enough to consider one of the two senses of BC rotation to evaluate scalar properties, such as the opacity function, reaction probability, total cross section (σ), average translational $\langle E_T'\rangle$, vibrational $\langle E_V'\rangle$, and rotational $\langle E_R'\rangle$ energies in products, etc. The situation changes if vector properties have to be evaluated, but as the two conditions we are considering are closely related, it comes out that also their vector properties are strongly connected. Thus, for two-vector angular distributions, the properties that will be considered in more detail in this work, if the two vectors involved are of polar type, or of axial type, their angular distributions coincide for both senses of BC rotation. But, if they involve a polar and an axial vector, one of the angular distributions is the mirror of the other one. Hence, it is enough to consider a single sense of rotation for the reagent diatomic molecule to evaluate the properties we are interested. Nevertheless, as trajectory calculations do not demand in general a very large amount of computer time, excepting if systems are close to threshold or near-threshold regions, it is probably good to recomend to run trajectories taking into account both senses of rotation, at least for a representative set of initial conditions, as it will allow us to check the correctness of the Monte Carlo sampling.

In all, around three millions of trajectories have been calculated for each reaction. Batches of 50 000−100 000 trajectories were run for each initial condition (E_T, v, j, and kind of alignment) to be sure to furnish statistically significant distributions. About 1000−20 000 reactive trajectories have been obtained for each initial condition, depending on the reaction and conditions considered (e.g., an average value of 8500 reactive trajectories/condition results for the reaction with Cl). The QCT initial conditions explored, given as intervals of values, are the following: E_T (eV), 0.25−4.0 (Cl), 1.11−4.5 (Br), 1.84−5.0 (I); $v(H_2)$, 0−12; $j(H_2)$, 1−18; taking into account in all cases three different **k**−**j** initial alignments (⊥, II, and null). Moreover, to analyze in deeper detail the vector properties, particular attention has been payed to the initial conditions indicated in Figures 2 and 5−8. These sets of (E_T, v, j) conditions have allowed us to study in detail the reactivity of reactions 1−3 at "ordinary" conditions, namely low energy collisions (low E_T, v, and j values), and at "extreme" conditions, namely high energy collisions (one of the above indicated parameters has a large value and the other two have low values).

4. Scalar Properties

4.1. Opacity Function. The reaction probability as a function of initial impact parameter (opacity function: $P(b)$ vs b) for representative initial conditions of reactions 1−3 is shown in Figure 2. On the overall parallel alignment has a larger trend to react at higher b values than the other alignments, and for all conditions (E_T, v, j), although the $P(b)$ vs b shape may be different for each alignment, the same bmax results for all of them. As expected, b_{max} increases with E_T, and the increase of b_{max} with v and j correlates with the increase of "effective

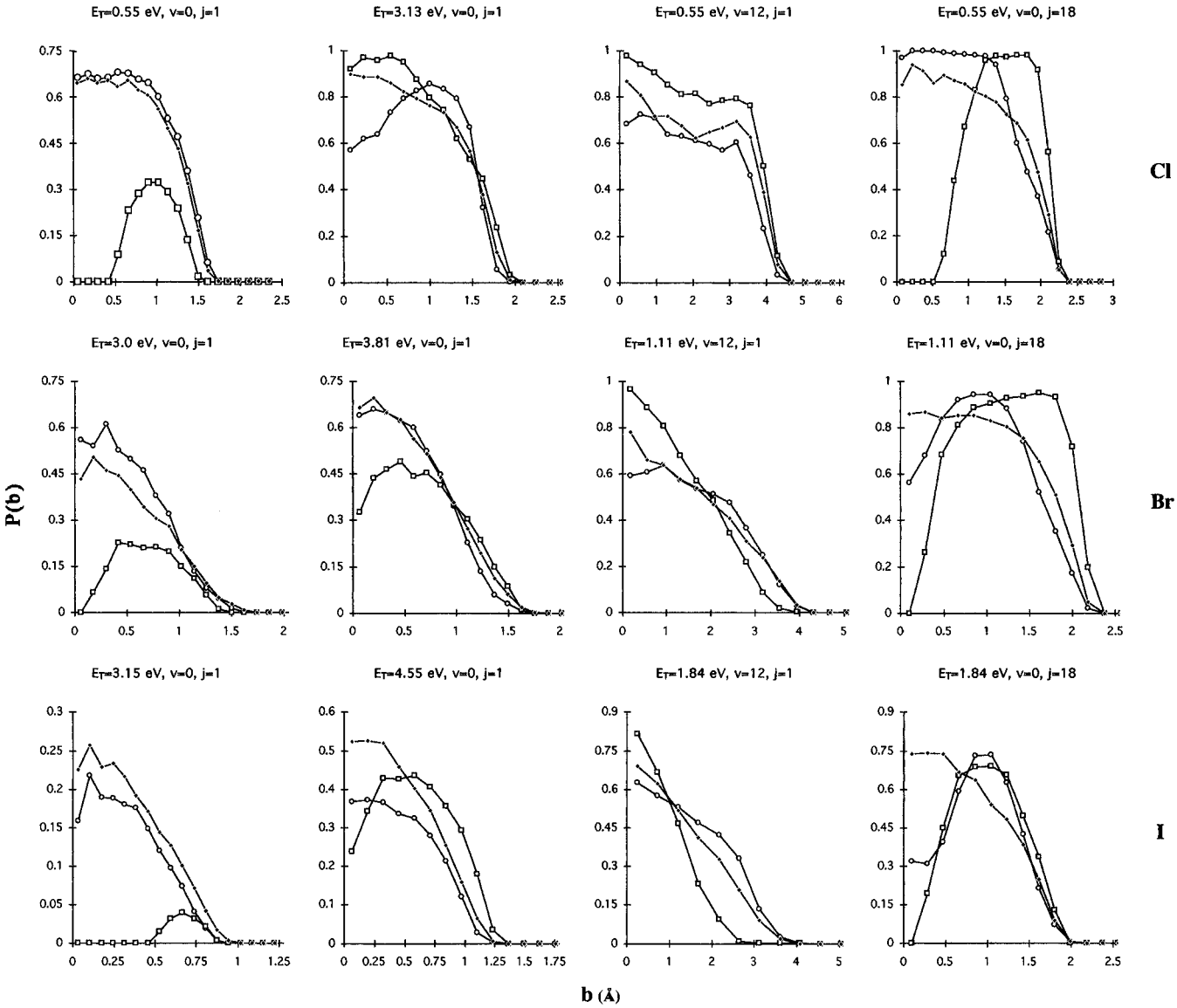

Figure 2. Opacity function ($P(b)$ vs b) for representative initial conditions (E_T, v, j, alignment) of reactions 1−3. The symbols "○", "□", and "◆" correspond to the results obtained for perpendicular, parallel and null alignments, respectively.

molecular size" (outer turning point) of the H_2 molecule as v and j increases, even though this correlation is stronger for the vibrational quantum number. At low E_T there is a marked tendency for reactive trajectories arising from parallel alignment to be produced preferently at higher impact parameters than in the case of the other alignments. However, the opacity functions tend to become similar as E_T increases. The opacity functions for all alignments become similar to each other quite rapidly as v increases. In the case of the j dependence, there is a tendency for reactive trajectories arising from parallel alignment to be produced preferently at higher impact parameters than in the case of the other alignments.

The opacity function dependence on the alignment can be understood on the basis of the collinear saddle point that exhibit the PES of reactions 1−3. As trajectories with initial parallel alignment have a tendency toward the insertion of the attacking atom into the reactant diatomic molecule bond (energetically unfavorable), in this case reactive trajectories will occur preferently at higher b values than for the other two alignments.

4.2. Excitation Function. The dependence of the total cross section (σ) on E_T, v, and j (excitation function) for representative initial conditions of reactions 1−3 is shown in Figure 3. The σ vs E_T dependence is the typical one for reactions that present a threshold energy, $E_{T,0}$.[22] This corresponds, as in our case, to reactions with a PES that presents a barrier between reactants and products. $E_{T,0}$ for parallel alignment is always higher than the ones for perpendicular and null alignments. But, although σ(II) is lower than $\sigma(\perp)$ and σ(null) at low and moderate E_T, for high enough E_T values σ(II) becomes larger than $\sigma(\perp)$ and σ(null).

Vibrational excitation of reactants typically enhances total cross sections,[23] and in fact this is also observed in almost all conditions, where σ increases almost linearly with v, except at very high v values (Figure 3). The vibrational enhancement of reactivity is particularly evident, as the presence of a late barrier in the PESs makes the H_2 vibrational energy particularly effective to overcome the barrier and reach the products valley, in agreement with what is expected from the Polanyi's rules.[24] In the v range of values explored σ(II) is in general equal or larger than $\sigma(\perp)$ and σ(null), and for all alignments the total cross section increases with v except at the higher v values, where a decrease with v is observed for reactions 2 and 3, that is more pronounced for parallel alignment. For reaction 1 a tendency toward saturation in the σ vs v dependence, with the presence of a plateau in the σ function, results at the higher v values explored for $\sigma(\perp)$ and σ(null), while σ(II) still exhibits

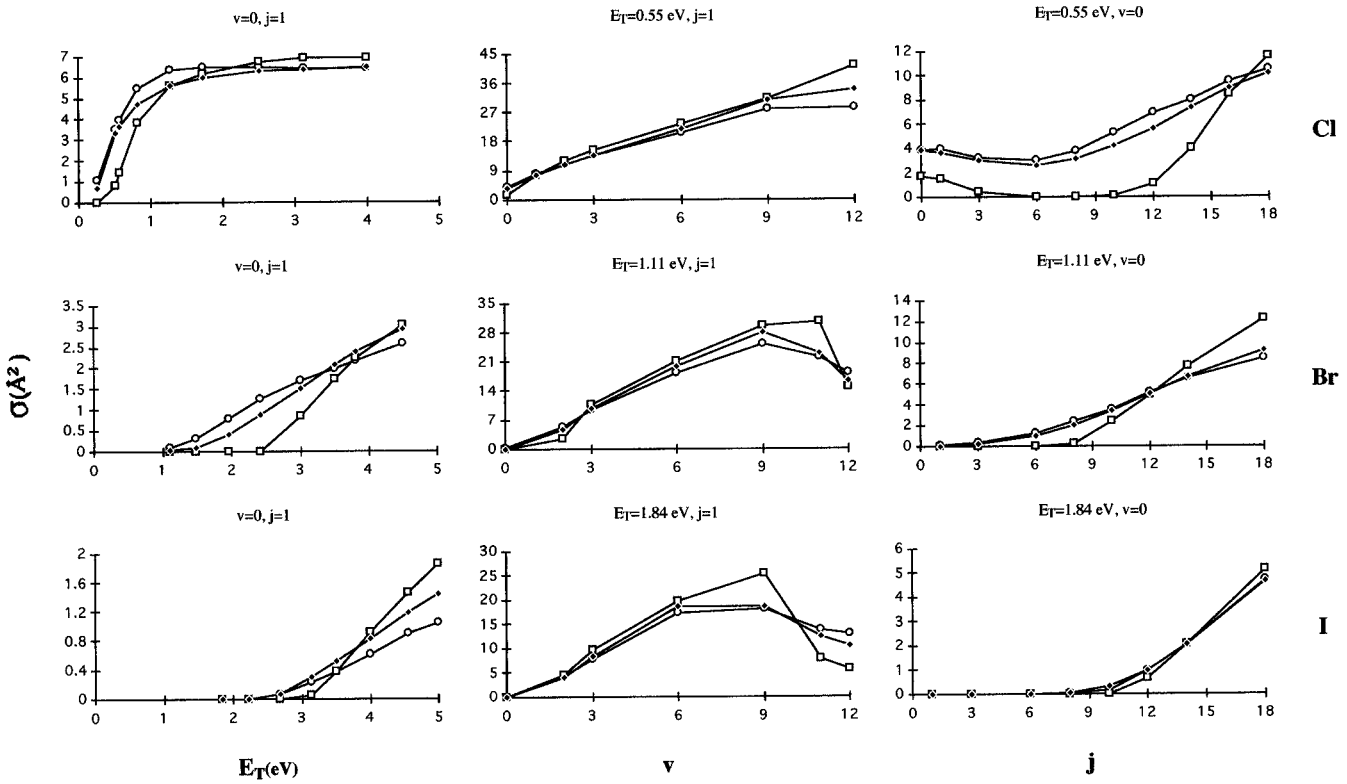

Figure 3. Total cross section (σ) for representative initial conditions (E_T, v, j, alignment) of reactions 1−3. Same comments as those in Figure 2.

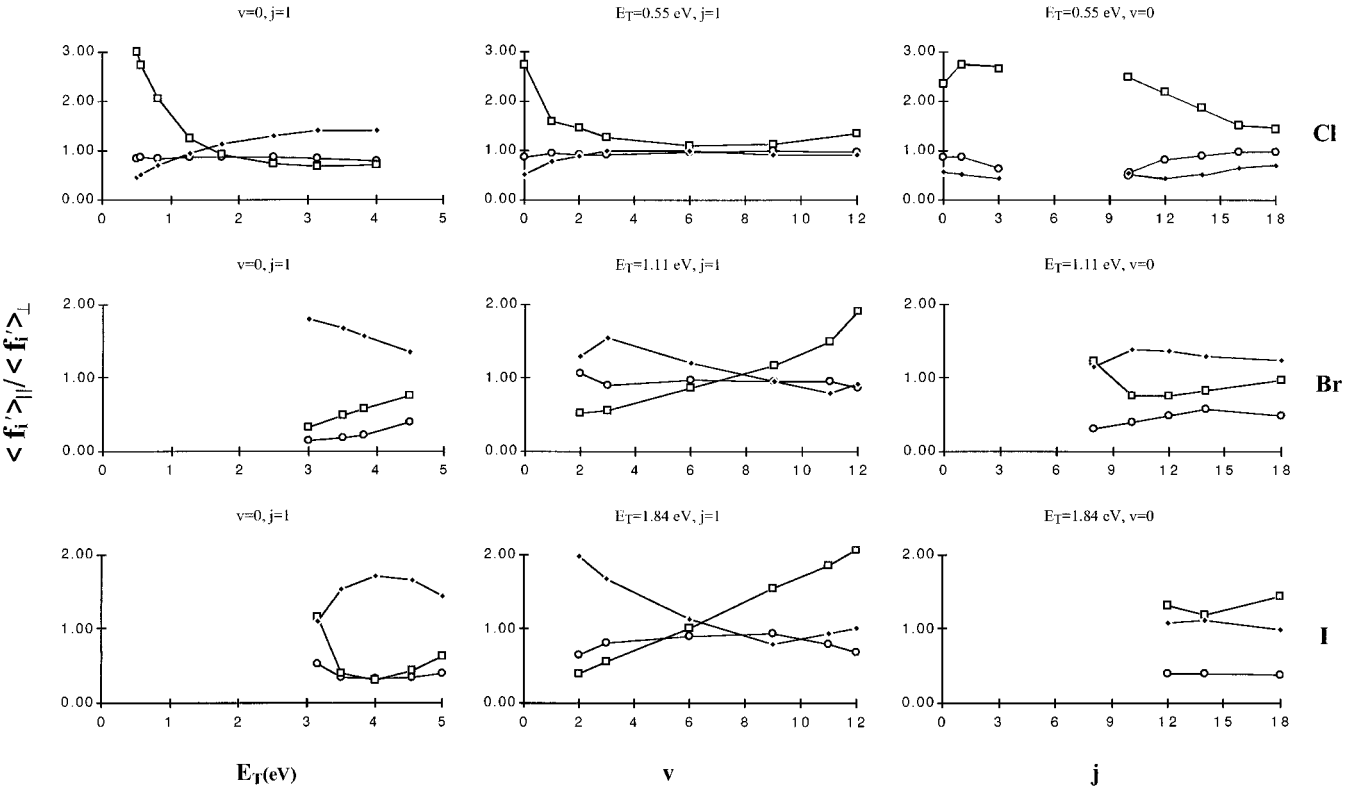

Figure 4. Ratio of average fractions of energy in products, $\langle f_i' \rangle_{II}/\langle f_i' \rangle_{\perp}$, for representative initial conditions (E_T, v, j, alignment) of reactions 1−3. The symbols "○", "□", and "◆" correspond to the results obtained for $\langle f_V' \rangle_{II}/\langle f_V' \rangle_{\perp}$, $\langle f_R' \rangle_{II}/\langle f_R' \rangle_{\perp}$, and $\langle f_T' \rangle_{II}/\langle f_T' \rangle_{\perp}$ respectively.

an increase with v. To the best of our knowledge there is a single case where a vibrational inhibition in a bimolecular reaction has been reported ($H + Li_2 \rightarrow LiH + Li$[25]). However, this case is very different to the ones treated here, as the $H + Li_2$ reaction presents a deep minimum between reactants and products and, although on the overall it conforms the general rule that vibrational excitation of a reagent bond promotes reaction,[23] this rule is contradicted when the collision energy and internal energy are low. For reactions 2 and 3, the tendency of σ to decrease in the region of the the higher v values treated results simply from the opening of the dissociative channel leading to X + H + H. This is a special case of collision induced dissociation (CID), because of the very high internal energy content of the reagent molecule. For reaction 1 the

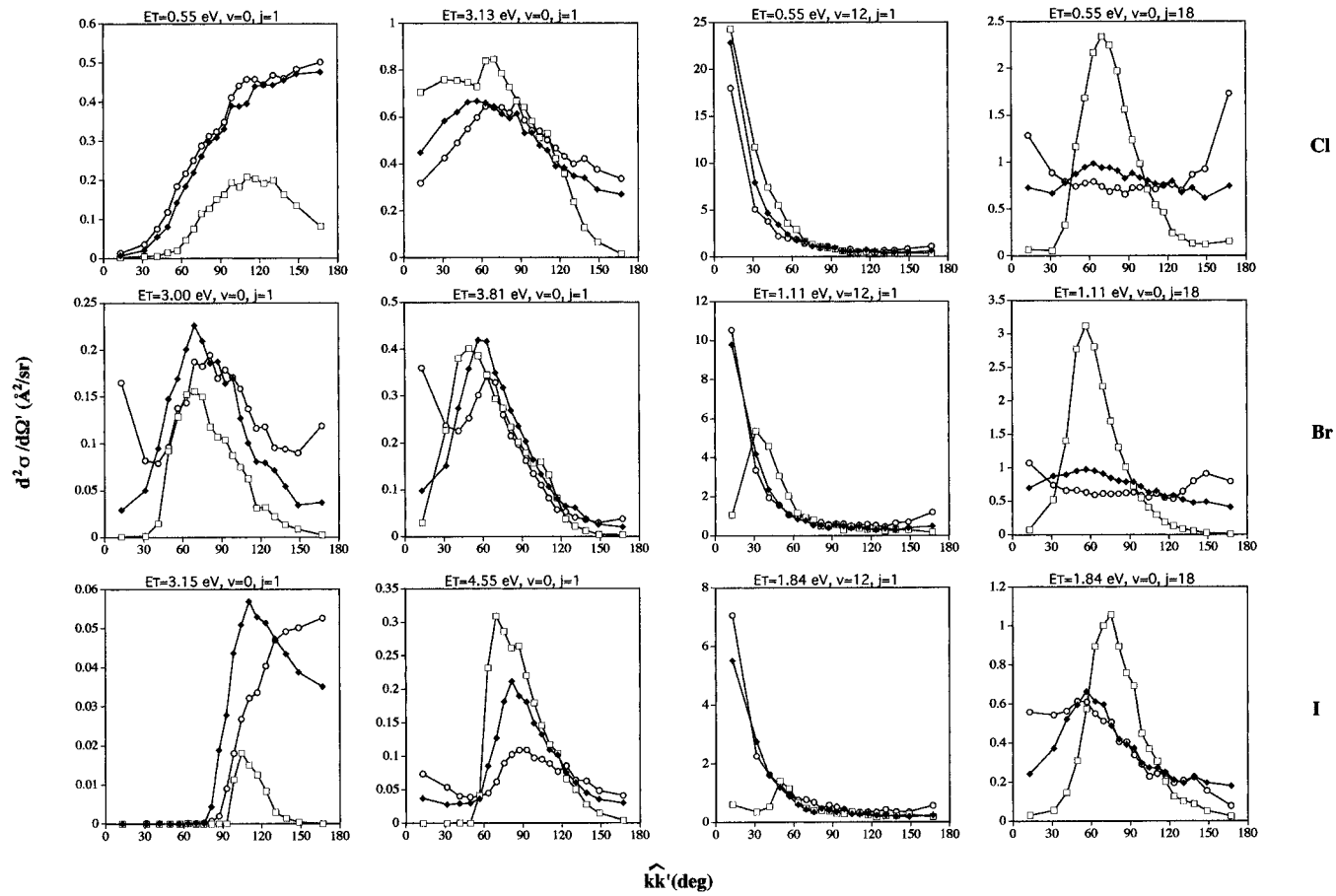

Figure 5. **kk′** angular distribution expressed in terms of the solid-angle differential cross section ($d^2\sigma/d\Omega'$) for representative initial conditions (E_T, v, j, alignment) of reactions 1−3. The symbols "○", "□", and "◆" correspond to the results obtained for perpendicular, parallel, and null alignments, respectively.

dissociative channel becomes also open at the higher v values considered but in a much less extension than for reactions 2 and 3.

The dependence of the total cross section on j presents typical shapes (Figure 3). For reaction 1, there is an initial decrease of σ with j that is followed by an increase at higher j values that can be interpreted as usually, on the basis on an initially dominant orientation effect that later, at higher j values, is substituted by a dominant energetic effect.[18,26−28] For reactions 2 and 3, there is a monotonic increase of σ with j that can be interpreted on the basis of a purely dominant energetic effect. For all reactions, σ(II) is initially below $\sigma(\perp)$ and σ(null), but for high enough j values, analogously to what happens in the σ vs E_T dependence, σ(II) becomes larger than $\sigma(\perp)$ and σ(null).

If the initial condition (E_T, v, j) is not very close to the threshold region for reactions to be produced, $^1/_3\sigma(\mathrm{II}) + {}^2/_3\sigma(\perp)$ provides a very good estimate to σ(null), the fully orientation averaged total cross section. This can be justified on the basis that from the three right-hand-side orthogonal space fixed axis available, one (Z axis) is involved in parallel alignment, while the other two (X and Y axis) are involved in perpendicular alignment.

The excitation function behaviour can be interpreted from the corresponding opacity functions, as the former are obtained after proper integration of the later properties.[22] Perpendicular alignment behaves in a more similar way to null alignment than the parallel one as it can be seen from the opacity functions. Hence, this fact should also be observed in the case of the excitation functions, as in fact it occurs. From the opacity function analysis it is also clear that for a given condition (E_T, v, j) the difference, if any, between the σ values of the different alignments arises exclusively from the reaction probability, as all them exhibit the same b_{max} values. In what respects to the larger threshold energies obtained for parallel alignment this directly correlates with the existence of a collinear saddle point in the PES of reactions 1−3 and to the fact that parallel alignment shows a tendency toward insertion (energetically unfavorable), not present for the other alignments. Because of this, with the exception of what occurs at high E_T or for excited vibrational levels of H_2, reactivity at low (very low) impact parameters is small (very small) compared to the one for the other alignments. For instance, in reaction 1, X = Cl, with E_T = 0.55 eV and H_2 ($v = 0$, and $j = 1$, 3 and 18), in the b interval 0−0.5 Å, $P(b, \mathrm{II})$ is equal to zero while $P(b, \perp)$ and $P(b, \mathrm{null})$ are almost constant and very similar: around 0.7, 0.7, and 0.9−1.0, respectively.

Previous arguments only remain on a merely geometrical point of view (i.e., we are leaving out considerations about the possible influence of the PES on orienting/reorienting the X + H_2 system during the collision). From this perspective, it is easier for an X atom to approach the H_2 molecule with angles near to insertion into the diatomic bond when **j** is initially prepared aligned parallel to **k** (side-on attack) than if **j** is initially prepared aligned perpendicular to **k** (end-on attack). We have also assumed in these considerations that the XHH arrangements in the strong interaction region (zone where interatomic distances are of the order of chemical bond distances) somewhat reflects the initial **k**−**j** alignment. Similar considerations were used previously with quite good success to rationalize the experimental and QCT results corresponding to the K + HF → KF + H[10] prototypic H−H−L system.

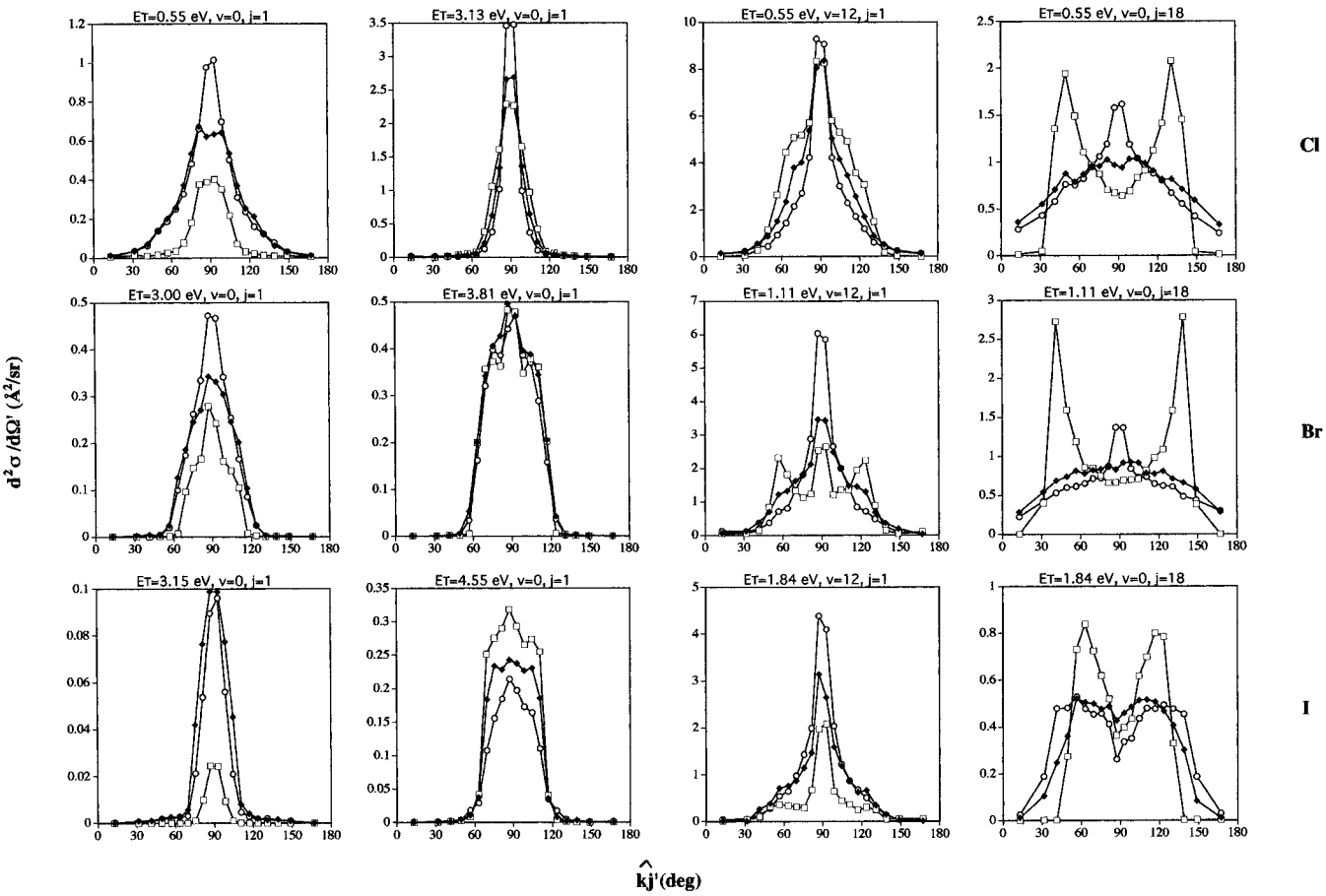

Figure 6. **kj′** angular distribution expressed in terms of the solid-angle differential cross section ($d^2\sigma/d\Omega'$) for representative initial conditions (E_T, v, j, alignment) of reactions 1−3. Same comments as those in Figure 5.

4.3. Average Fraction of Energy in Products. Even though regarding scalar properties we have been mainly concerned with reactivity (i.e.,with the total cross section), for completeness some insight on the average fraction of energy in products has been performed. To make easier the comparison between the influence of perpendicular and parallel alignments on the average fractions of energies available in products, the $\langle f_i'\rangle_{II}/\langle f_i'\rangle_{\perp}$ ratio has been plotted in Figure 4.

Reaction 1 behaves in a different manner than do reactions 2 and 3, and the latter reactions behave similarly to each other. The much closer vicinity to the products arrangement of the saddle point for reactions 2 and 3 compared to the case for reaction 1 is probably the main reason of the different behaviour obtained for these systems. Thus, although the X−H distance at the saddle point is in all cases quite close to the corresponding equilibrium distance in the X−H product diatomic molecule: 1.273 (1.401), 1.414 (1.476), and 1.609 (1.634) Å, respectively for X = Cl, Br, and I, where between parentheses the X−H distance for each saddle point is given, the H−H distance at the saddle point (0.990, 1.207, and 1.528 Å, respectively, for X = Cl, Br, and I) substantially differs from the corresponding equilibrium distance in the H_2 molecule (0.741 Å). From the energetics and consistently with geometrical results, it comes out that the barrier height including the zero point energy ($\Delta E^{\neq} + \Delta ZPE$) and the reaction energy (ΔE) are equal to 0.244, 0.766, and 1.502 eV and 0.130, 0.810, and 1.551 eV for reactions 1−3, respectively. The geometries of the XHH saddle points and energetics have been taken from refs 11 (X = Cl), 13 (X = Br), and 14 (X = I).

For reaction 1, $\langle f_V'\rangle_{II}/\langle f_V'\rangle_{\perp}$, is almost constant and close to the unity, except for what happens when the dependence on j is considered, as between $j = 6$ and 9, where there are no reactive trajectories for parallel alignment. But disregarding these j values interval, the abovementioned statement on the ratio for vibration is also valid here. $\langle f_R'\rangle_{II}/\langle f_R'\rangle_{\perp}$ is greater than one and tends to decrease as E_T, v, or j increase. $\langle f_T'\rangle_{II}/\langle f_T'\rangle_{\perp}$ lies approximately between 0.5 and 1.3, being in general almost constant (for the v and j dependences) or showing an increase (for the E_T dependence). For the most representative "ordinary" condition leading to reaction 1 for all alignments ($E_T = 0.55$ eV and H_2 ($v = 0, j = 1$)), the three ratios of fractions take the following values: 0.86 (V), 2.72 (R), and 0.50 (T), respectively (Figure 4).

For reactions 2 and 3, in general $\langle f_V'\rangle_{II}/\langle f_V'\rangle_{\perp}$ is essentially constant, and the most significative changes occur for $\langle f_R'\rangle_{II}/\langle f_R'\rangle_{\perp}$ and $\langle f_T'\rangle_{II}/\langle f_T'\rangle_{\perp}$. Thus, while the former ratio tends to increase (in some cases, after an initial decrease), the latter one tends to decrease (in some cases, after an initial increase). For the most representative "ordinary" condition leading to reaction 2 for all alignments ($E_T = 3.0$ eV and H_2 ($v = 0, j = 1$)), the ratios take the following values: 0.13 (V), 0.32 (R), and 1.80 (T), respectively. Analogously, for the most representative "ordinary" condition for reaction 3 ($E_T = 3.15$ eV and H_2 ($v = 0, j = 1$)), the ratios take the following values: 0.53 (V), 1.14 (R), and 1.10 (T), respectively.

5. Vector Properties

The **kk′**, **kj′**, **k′j′**, and **l′j′** angular distributions for representative initial conditions of reactions 1−3, that is to say from "ordinary" to "extreme" conditions (cf. in section 3), are plotted in Figures 5, 6, 7, and 8, respectively, expressed in terms of the solid-angle differential cross section ($d^2\sigma/d\Omega'$). To calculate this property the uniform phase space (UPS) method[29] has been

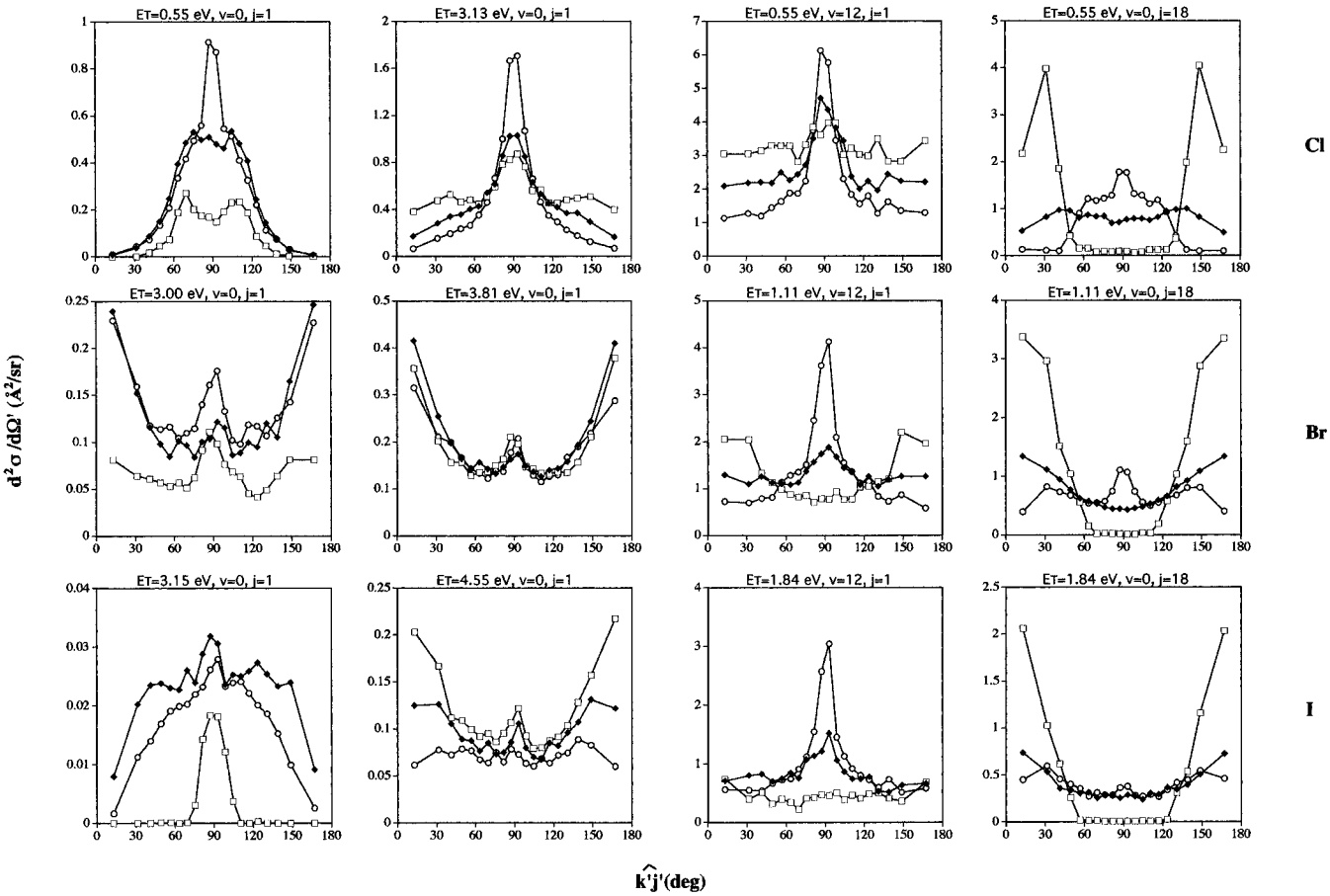

Figure 7. $\mathbf{k'j'}$ angular distribution expressed in terms of the solid-angle differential cross section ($d^2\sigma/d\Omega'$) for representative initial conditions (E_T, v, j, alignment) of reactions 1−3. Same comments as those in Figure 5.

used to construct the histograms. Thus, the 0−180° angular range has been divided into 20 bins, in such a way that each bin contains an equal volume of phase space: distribution uniform in the solid angle (Ω') but not in the angle formed by the two vectors (θ'). In Figures 5−8 the value of ($d^2\sigma/d\Omega'$) for each bin is specified at the center of the interval. The forward/backward (f/b) (parallel/antiparallel (p/ap)) scattering ratio of the $\mathbf{kk'}$ ($\mathbf{kj'}$, $\mathbf{k'j'}$ and $\mathbf{l'j'}$) angular distribution considered in the next subsections are equal to the $N_r(\theta' < 90°)/N_r(\theta' > 90°)$ ratio, where $N_r(\theta' < 90°)$ ($N_r(\theta' > 90°)$) is the number of reactive trajectories obtained for each initial condition at θ' angles lower (higher) than 90°. Analogously as occurred in the case of scalar properties, for the two-vector properties described in this section it will be shown that the results obtained for perpendicular alignment are closer to the ones for random (null) alignment, than those in the case of parallel alignment.

The angular momentum transfer when evolving from reactants to products has a different behaviour depending on the kinematics (mass combinations) of the reactions considered. Reactions 1−3 are of the H−L−L type and for the conditions considered it comes out that, except for high j values, a $l \rightarrow l'$ transformation trend has been observed for all alignments. However, in general this tendency is not strong. In the high j case, neither the $l \rightarrow l'$ nor the $l \rightarrow j'$ transformation trends have been observed.

5.1. kk′ Angular Correlation. The $\mathbf{kk'}$ differential cross section is plotted in Figure 5. This distribution is predominantly backward for the lowest E_T value considered in each system ($E_{T,min}$) and H_2 ($v = 0, j = 1$), but as E_T increases the distribution becomes symmetrical, and at the higher E_T values considered the forward scattering clearly dominates, with the exception of what happens for two alignments of reaction 3. In this case, the $\mathbf{kk'}$ angular distribution is nearly symmetrical for perpendicular and null alignments. For H_2 ($v = 0$), the lowest v value taken into account, with E_T and j fixed at their lowest values considered ($E_{T,min}$, $j = 1$), the $\mathbf{kk'}$ scattering is predominantly backward, but as v increases it becomes rapidly predominantly forward. For H_2 ($j = 1$), the lowest j value taken into account, with E_T and v fixed at their lowest values considered ($E_{T,min}$, $v = 0$), the $\mathbf{kk'}$ scattering is predominantly backward, but as j increases it becomes progressively more forward, and in general it is predominantly forward for H_2 ($j = 18$). This behavior is more apparent for parallel alignment. In general, when reactivity is comparable for all alignments, the shape of the $\mathbf{kk'}$ distributions is similar in all cases, with the only exception of what happens at high j values. Concretely (e.g., for ($E_{T,min}$, $v = 0, j = 18$)), while the $\mathbf{kk'}$ distribution is very/quite broad for perpendicular and null alignments, for the parallel case it presents a rather sharp maximum inside the 60−90° $\mathbf{kk'}$ angular interval.

The influence of E_T on the $\mathbf{kk'}$ distribution can be interpreted on the basis of a purely impulsive effect, assuming that the effect of more repulsive parts of the PES energetically accessible as E_T increases can not counterbalance it. The influence of the H_2 vibrational quantum level on the $\mathbf{kk'}$ scattering can be interpreted on the basis of the relaxation produced in the H-H bond as v increases. As indicated in section 4.1., an increase of "effective molecular size", directly related to the outer turning point of the H_2 molecule, is produced as v and j increases, even though the increase is stronger for the vibrational quantum numbers. This fact could facilitate the abstraction at larger distances of a hydrogen atom from the hydrogen molecule by the attacking halogen atom, thus favoring the forward scattering. The influence of the H_2 rotational quantum level on $\mathbf{kk'}$ can be interpreted in a similar way as in the case of the effect of v,

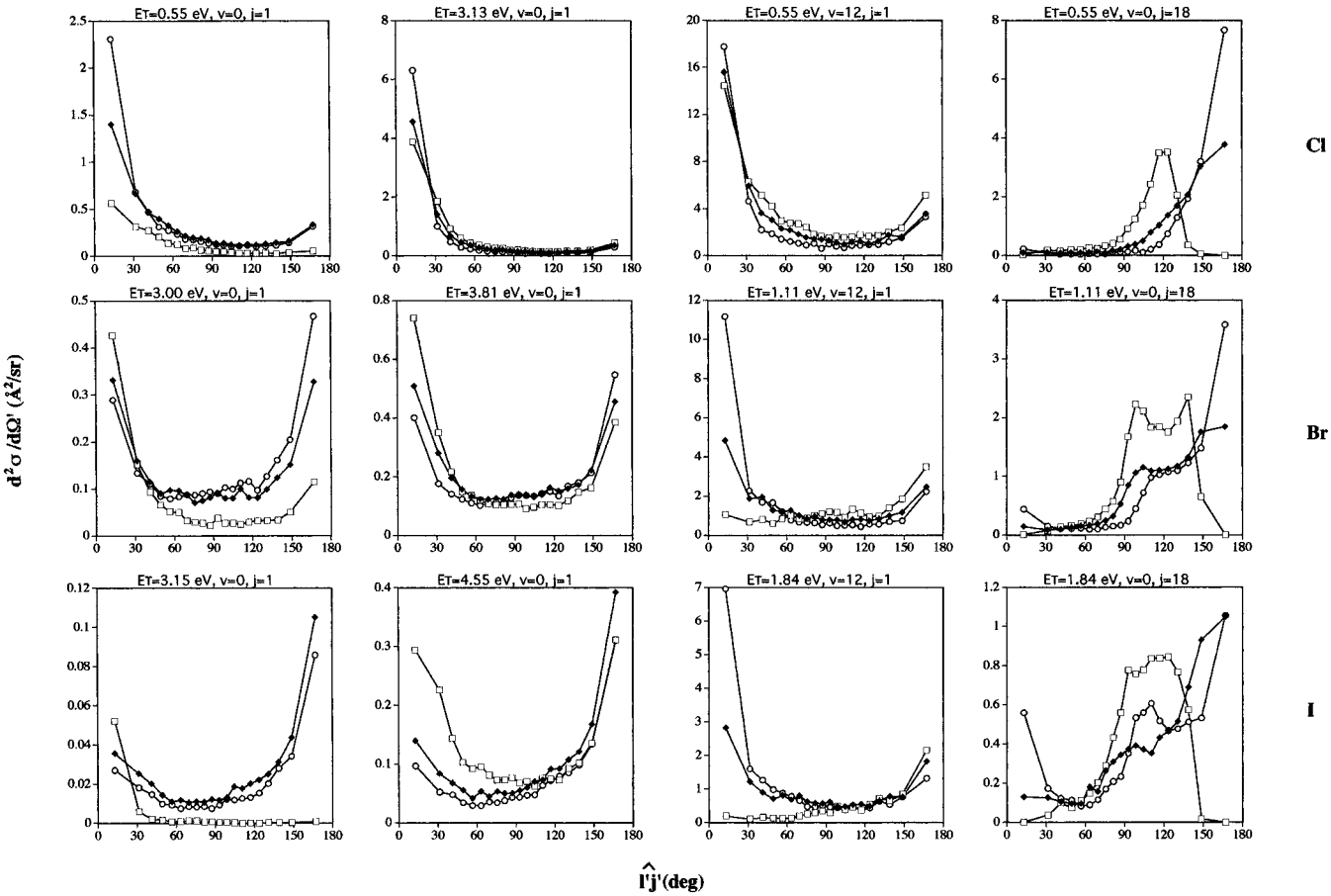

Figure 8. **l′j′** angular distribution expressed in terms of the solid-angle differential cross section ($d^2\sigma/d\Omega'$) for representative initial conditions (E_T, v, j, alignment) of reactions 1−3. Same comments as those in Figure 5.

even though as mentioned before the influence of j on the H_2 outer turning point value is not so high as in the case of v and also taking into account the existence of rovibrational coupling.

5.2. kj′ Angular Correlation. The **kj′** differential cross section (Figure 6) is symmetrical around 90° for all initial conditions. Thus, $\langle \mathbf{kj'} \rangle = 90°$, the p/ap scattering ratio is within the 0.93−1.10 interval, and the first-order orientation parameter is very close to zero ($A_0^{(1)}(\mathbf{k}\cdot\mathbf{j'})$: 10^{-4}−10^{-2} in absolute value). The shape of the **kj′** angular distribution is similar for H_2 ($v = 0$, $j = 1$) and for ($E_{T,min}$, H_2 ($j = 1$)), respectively, within the E_T and v intervals considered. Except for what happens at high j values, the **kj′** distribution shows a maximum at 90° for all alignments. The most remarkable effect occurs when the dependence of the **kj′** distribution on j is considered. Here the **kj′** distribution is broader than in the abovementioned cases, and although it is also symmetrical around 90°, instead of a maximum peaking at 90°, a minimum appears at this angle for parallel alignment at high enough j values. In this situation, two maxima symmetrically placed around 90° are present (e.g., for the initial condition ($E_{T,min}$, H_2 ($v = 0, j = 18$)) both maxima in $d^2\sigma/d\Omega'$ occur at around 45 and 135° for reactions 1 and 2, and at around 60° and 120° for reaction 3. It is worth noting that for this last reaction a similar but smoother behavior is also observed for perpendicular alignment, and a wide plateau showing slightly this tendency also appears in the case of null alignment.

The just-mentioned behaviour exhibited by reactive trajectories that arise from parallel alignment directly correlates with the specification of the initial conditions. Thus, the reactive trajectories that peak at an angle lower than 90° or are placed around it correspond to the ones arising from an initial situation where vectors **k** and **j** are antiparallel (**kj** angle = 180°). By contrary, the reactive trajectories that peak at an angle higher than 90° or are placed around it correspond to the ones arising from an initial situation where vectors **k** and **j** are parallel (**kj** angle = 0°). These two initial angular arrangements of vectors **k** and **j** correspond to two different orientations of them but to a single aligment case and concretely to the parallel one. The behavior exhibited by perpendicular alignment in reaction 3 for high j values is not easy to understand, and it is even more evident for H_2 ($v = 0$, $j = 14$) than for H_2 ($v = 0$, $j = 18$). In what respects to the reason because **j′** tends to be perpendicular to **k**, after consideration of the angular momenta transformation from reactants to products at the beginning of this section, it becomes clear that this is not a trivial result coming from kinematics.

5.3. k′j′ Angular Correlation. The same comments on the **kj′** angular distribution are also valid here, for example, the **k′j′** angular distribution (Figure 7) is symmetrical around 90° ($\langle \mathbf{k'j'} \rangle = 90°$), the p/ap ratio is within the 0.93−1.10 interval, and the first-order orientation parameter is very close to zero ($A_0^{(1)}(\mathbf{k'}\cdot\mathbf{j'})$: 10^{-4}−10^{-2} in absolute value). However, for **k′j′** the angular distributions are much broader than the ones for **kj′**, and the symmetrical two maxima that appear for parallel alignment and high j values now occur at lower and higher angles than those for **kj′**, respectively.

5.4. l′j′ Angular Correlation. The **l′j′** differential cross section is plotted in Figure 8. For reaction 1, except for what happens for parallel alignment, the p/ap scattering ratio increases notably with E_T, but for the former alignment this ratio is almost constant. For perpendicular and parallel alignments, the p/ap ratio decreases notably with v, but for null alignment it is almost constant. For this reaction the most remarkable effect takes place when the **l′j′** angular dependence on j is accounted for.

Thus, although the $\mathbf{l}'\mathbf{j}'$ angular distribution is predominantly parallel for the lower j values considered, as j increases both vectors tend to be antiparallel. The p/ap ratio decreases with j in a very important way (e.g., for H_2 ($v = 0$, $j = 18$) there is a very small number of reactive trajectories with $\mathbf{l}'\mathbf{j}'$ angles lower or equal to 90°).

For reaction 2, the p/ap scattering ratio is almost constant within the 3.0−3.81 eV E_T interval and H_2 ($v = 0$, $j = 1$). For perpendicular and null alignments, the p/ap ratio increases notably with v, but for parallel alignment an important decrease in this ratio results. As in reaction 1, here the most remarkable effect also occurs when the $\mathbf{l}'\mathbf{j}'$ angular dependence on j is accounted for.

For reaction 3, and perpendicular and null alignments, the p/ap scattering ratio is essentially constant (approximately equal to 0.5) and $\langle \mathbf{l}'\mathbf{j}' \rangle$ is around 110°, in the 3.15−4.55 eV E_T range and H_2 ($v = 0$, $j = 1$). But for parallel alignment, the p/ap ratio strongly decreases with E_T and is equal to 22.9 and 1.2 with $\langle \mathbf{l}'\mathbf{j}' \rangle = 26$ and 87° for E_T values of 3.15 and 4.55 eV, respectively. As v increases, this ratio substantially increases for perpendicular an null alignments and decreases for parallel alignment, being equal to 2.5, 1.4 and 0.3 with $\langle \mathbf{l}'\mathbf{j}' \rangle = 62°$, 82°, and 120°, respectively, for $E_T = 1.84$ eV and H_2 ($v = 12$, $j = 1$). As in reactions 1 and 2, both vectors tend to become antiparallel as j increases, being also here a remarkable effect.

6. Summary and Conclusions

The next set of reactions have been considered in this work: $X + H_2$ (X = Cl, Br, and I), using the QCT method. These reactions may be taken as models for endoergic triatomic reactions with H−L−L kinematics and a collinear saddle point. In this contribution, mainly devoted to the stereodynamics, a very large number of trajectories have been calculated to study the dependence of scalar and vector properties on (E_T, v, j), as well as the effect of considering perpendicular (⊥), parallel (II), and random (null) initial $\mathbf{k}-\mathbf{j}$ alignment. The threshold energy for parallel alignment is always higher than the ones for perpendicular and null alignments. But, although σ(II) is lower than $\sigma(\perp)$ and σ(null) at low and moderate E_T, for high enough E_T values σ(II) becomes larger than $\sigma(\perp)$ and σ(null). In the v range of values explored $\sigma(\|)$ is in general equal or larger than $\sigma(\perp)$ and σ(null), and for all alignments the total cross section increases with v except at the higher v values. For all reactions σ(II) is initially below $\sigma(\perp)$ and σ(null), but for high enough j values, analogously to what happens in the σ vs E_T dependence, σ(II) becomes larger than $\sigma(\perp)$ and σ(null). These results and others concerning scalar properties may be explained taking into account the saddle point properties for each reaction and the geometrical implications of the different types of alignments. Some simple relations to simplify the QCT calculations when considering the case of parallel alignment have also been indicated, and we have also shown that $^1/_3\sigma(\text{II}) + {}^2/_3\sigma(\perp)$ provides a very good estimate to σ(null), if the system is not close to the threshold region. For the two-vector properties considered, as in the case of scalar properties, the results obtained for perpendicular alignment are in general closer to the ones for null alignment than the results obtained for parallel alignment. The dependences of the angular distributions ($\mathbf{k}$, $\mathbf{k}'$), ($\mathbf{k}$, $\mathbf{j}'$), ($\mathbf{k}'$, $\mathbf{j}'$), and ($\mathbf{l}'$, $\mathbf{j}'$) on (E_T, v, j) as well as on the alignments can be interpreted taking into account the increase of "effective molecular size" produced when the H_2 molecule is rovibrationally excited, and the fact that it is easier for an X atom to approach the H_2 molecule with a situation near to insertion for parallel alignment (side-on attack) than for the perpendicular one (end-on attack). The angular correlations that result from the calculation are not a trivial result coming from a kinematic constraint, being particularly remarkable the role played by the rotational angular momentum of the H_2 molecule on them.

Additional information on the data contained in this work and about other results not included (average angles, f/b and p/ap ratios, first- ($A_0^{(1)}$) and second-order ($A_0^{(2)}$) orientation and alignment parameters, differential polar cross sections, etc.) is available from the authors upon request.

Acknowledgment. This work has been supported by the Dirección General de Enseñanza Superior (D.G.E.S.) of the Spanish Ministry of Education and Culture through the Projects PB92-0756, PB95-0598-C02-01 and PB95-0598-C02-02. J.D.S. thanks the University of la Rioja for partial financial support (ref. 96PYA37JSM) of his Ph.D. thesis. We are also grateful to Prof. Donald G. Truhlar and Dr. Tom C. Allison for sending us the codes of the PESs for H_2Cl and H_2Br.

References and Notes

(1) Orr-Ewing, A. J.; Zare, R. N. *Annu. Rev. Phys. Chem.* **1994**, *45*, 315.

(2) Loesch, H. J. *Annu. Rev. Phys. Chem.* **1995**, *46*, 555.

(3) *J. Phys. Chem.* **1995**, *99*, 13569.

(4) Barnwell, J. D.; Loeser, J. G.; Herschbach, D. R. *J. Phys. Chem.* **1983**, *87*, 2781.

(5) Kim, S. K.; Herschbach, D. R. *Faraday Discuss.* **1987**, *84*, 159.

(6) Huber, K. P.; Herzberg, G. *Molecular Spectra and Molecular Structure. IV. Constants of Diatomic Molecules*; Van Nostrand Reinhold: New York, 1979.

(7) Loesch, H. J.; Remscheid, A.; Stenzel, E.; Stienkemeier, F.; Wüstenbecker, B. In *Physics of Electronic and Atomic Collisions*; MacGillivray, W. R., McCarthy, I. E., Standage, M. C., Eds.; Adam Hilger: Bristol, 1992; p 579.

(8) Loesch, H. J.; Stienkemeier, F. *J. Chem. Phys.* **1993**, *98*, 9570.

(9) Pattengill, M. D.; Zare, R. N.; Jaffe, R. L. *J. Phys. Chem* **1987**, *91*, 5489.

(10) González, M.; Gilibert, M; Aguilar, A.; Sayós, R. *Chem. Phys.* **1995**, *200*, 289.

(11) Allison, T. C.; Lynch, G. C.; Truhlar, D. G.; Gordon, M. S. *J. Phys. Chem.* **1996**, *100*, 13575.

(12) Alagia, M; Balucani, N; Cartechini, L.; Casavecchia, P; van Kleef, E. H.; Volpi, G. G.; Aoiz, F. J.; Bañares, L.; Schwenke, D. W.; Allison, T. C.; Mielke, S. L.; Truhlar, D. G. *Science* **1996**, *273*, 1519.

(13) Lynch, G. C.; Truhlar, D. G.; Brown, F. B.; Zhao, J.-G. *J. Phys. Chem.* **1995**, *99*, 207.

(14) González, M.; Hijazo, J.; Sayós, R. To be submitted.

(15) González, M. *Faraday Discuss.* **1991**, *91*, 339.

(16) Kliner, D. A. V.; Rinnen, K.-D.; Buntine, M. A.; Adelman, D. E.; Zare, R. N. *J. Chem. Phys.* **1991**, *95*, 1663.

(17) Aker, P. M.; Germann, G. J.; Valentini, J. J. *J. Chem. Phys.* **1990**, *90*, 4795.

(18) Mayne, H. R. *Int. Rev. Phys. Chem.* **1991**, *10*, 107.

(19) González, M.; Gilibert, M.; Aguilar, A.; Sayós, R. *J. Chem. Phys.* **1993**, *98*, 2927.

(20) Gilibert, M.; Aguilar, A.; González, M.; Sayós, R. *J. Chem. Phys.* **1993**, *99*, 1719

(21) Sayós, R.; González, M.; Gilibert, M. TRIQCT Unpublished program.

(22) Levine, R. D.; Bernstein, R. B. *Molecular Reaction Dynamics and Chemical Reactivity*; Oxford University Press: Oxford, 1987; Chapter 2.

(23) Polanyi, J. C. *Science* **1987**, *236*, 680.

(24) Polanyi, J. C. *Acc. Chem. Res.* **1972**, *5*, 161.

(25) Kim, S. K.; Jeoung, S. C.; Tan, A. L.-C.; Herschbach, D. R. *J. Chem. Phys.* **1991**, *95*, 3854.

(26) Sathyamurthy, N. *Chem. Rev.* **1983**, *83*, 601.

(27) Grote, W.; Hoffmeister, M.; Schleysing, R.; Zerhau-Dreiöfer, H.; Loesch, H. J. In *Selectivity in Chemical Reactions*; Whitehead, J. C., Ed.; Kluwer: Dordrecht, 1988; p 47.

(28) González, M.; Gilibert, M.; Aguilar, A.; Sayós, R. *Chem. Phys. Lett.* **1993**, *204*, 578.

(29) Truhlar, D. G.; Muckerman, J. T. In *Atom-Molecule Collision Theory: A Guide for the Experimentalist*; Bernstein, R. B., Ed.; Plenum Press: New York, 1979; Chapter 16.